

Approximation with Error Bounds in Spark

Technical Report DCS-TR-731, 12/3/2018

Guangyan Hu
Rutgers University
New Brunswick, NJ
gh279@cs.rutgers.edu

Desheng Zhang
Rutgers University
New Brunswick, NJ
d.z@cs.rutgers.edu

Sandro Rigo
University of Campinas
Campinas - SP, Brazil
srigo@unicamp.br

Thu D. Nguyen
Rutgers University
New Brunswick, NJ
tdnguyen@cs.rutgers.edu

Abstract—We introduce a sampling framework to support approximate computing with estimated error bounds in Spark. Our framework allows sampling to be performed at the beginning of a sequence of multiple transformations ending in an aggregation operation. The framework constructs a data provenance graph as the computation proceeds, then combines the graph with multi-stage sampling and population estimation theories to compute error bounds for the aggregation. When information about output keys are available early, the framework can also use adaptive stratified reservoir sampling to avoid (or reduce) key losses in the final output and to achieve more consistent error bounds across popular and rare keys. Finally, the framework includes an algorithm to dynamically choose sampling rates to meet user specified constraints on the CDF of error bounds in the outputs. We have implemented a prototype of our framework called ApproxSpark, and used it to implement five approximate applications from different domains. Evaluation results show that ApproxSpark can (a) significantly reduce execution time if users can tolerate small amounts of uncertainties and, in many cases, loss of rare keys, and (b) automatically find sampling rates to meet user specified constraints on error bounds. We also explore and discuss extensively trade-offs between sampling rates, execution time, accuracy and key loss.

Index Terms—Spark, approximation, multi-stage sampling, stratified sampling

I. INTRODUCTION

Data driven discovery has become critical to the missions of many enterprises and a scientific pillar. At the same time, the rate of data production and collection is outpacing technology scaling, implying that significant future investment, time, and energy will be needed for data processing [1]. Approximate computing is a powerful tool to reduce these processing needs. Many data analytic applications such as machine learning and log processing are amenable to approximation (e.g., [2]–[4]). As a concrete example, suppose a company wants to know the age distribution of its customers for a particular product. In such an application, estimated counts derived from data samples may be sufficient, allowing tradeoffs between precision and processing time and/or cost.

In this paper, we propose and evaluate a sampling framework for creating and running a class of approximate Spark [5] programs that can compute estimated values with error bounds (i.e., confidence intervals). Today’s pipeline for massive data processing often includes multiple steps of data transformations [6], [7], which complicates the error bound estimation process. However, having estimated error bounds is important

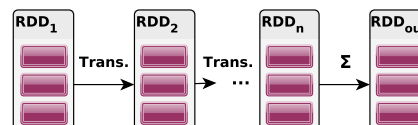


Fig. 1: A Spark computation comprising a sequence of transformations followed by an aggregation operation.

because it allows users to intelligently balance precision and performance metrics such as execution time and/or energy consumption. Spark is one of several popular data processing systems that have been widely adopted in different domains [8]–[11]. Embedding a general approximation framework in Spark will make approximation easily accessible to application developers in many different fields. In addition, while our work is specific to Spark, it should be portable to other DAG-based data processing systems.

Consider a Spark computation that is a sequence of operations (i.e., transformations) ending with an aggregation operation (e.g., sum) as shown in Figure 1. If we sample the resilient distributed dataset RDD_n immediately before the aggregation, then it is straightforward to use simple random sampling theories to estimate the sums and corresponding error bounds [12]. However, this is unlikely to reduce the amount of work required to complete the computation by very much, since the aggregation operation (e.g., sum) is relatively inexpensive. The challenge is thus to sample earlier, e.g., sample when creating RDD_1 , so that we can reduce the amount of I/O needed for reading in the input data and the work performed by multiple operations, while still being able to estimate the aggregate output values and corresponding error bounds.

The key insights behind our work include: (i) sampling at RDD_1 is equivalent to multi-stage sampling at RDD_n , so that multi-stage sampling theories can be used to estimate the aggregate output values and their error bounds, (ii) it is possible to build a data provenance graph to relate RDD_1 ’s population and the chosen sample to RDD_n ’s population and the resulting sample of RDD_n , and (iii) the data provenance graph can be combined with population estimation techniques to estimate all quantities, i.e., the number of clusters at each level and the number of items in sampled clusters, required by multi-stage sampling theories.

In Section III, we show how data provenance graphs can be constructed, and how to use the graphs to estimate the quantities needed to use the multi-stage sampling theories. Critically, we show how to account for the inaccuracies introduced by population estimations when estimating error bounds. For computations that produce multiple key-value pairs, and the final keys are known early in the transformation sequence, we show how adaptive stratified reservoir sampling (ASRS) [13] can be integrated with multi-stage sampling to avoid losing rare keys, as well as balance the sampling between popular and rare keys.

We have implemented the proposed framework in a prototype system called ApproxSpark (Section IV). Our framework supports a subset of common Spark transformations, including `map`, `flatMap`, `mapValues`, and `filter`, and aggregation operations such as average and sum. ApproxSpark can sample when the input data is being loaded into an RDD, or from an existing RDD, at both the partition level (i.e., choose a random subset of partitions) and the data item level (i.e., choose a random subset of data items within each chosen partition). When running an approximate computation, users have the flexibility to specify sampling rates or constraints on the CDF of relative error bounds for values associated with output keys—if the computation produces a single value or key-value pair, then the latter reduces to just the maximum allowable relative error bound. When the user specifies constraints for the error bound CDF, ApproxSpark will run pilot executions of several partitions and use the results to select appropriate sampling rates.

We note that Apache Spark already supports sampling of an RDD. However, the current implementation has several limitations and does not support estimating error bounds. We discuss this implementation in more detail in Section II.

We have used ApproxSpark to implement five approximate applications from different domains such as text mining, graph analysis, and log analysis. We use the applications to evaluate ApproxSpark and explore the tradeoffs between performance and inaccuracies. Among other findings, our results show that (i) ApproxSpark can significantly reduce execution time and/or energy consumption if users can tolerate small amounts of uncertainties and, in many cases, loss of rare keys; (ii) it is possible to automatically find sampling rates to meet user specified constraints on the CDF of error bounds in the output; (iii) partition sampling can lead to greater reduction in execution time than data item sampling, but lead to more key loss and significantly larger error bounds, especially for the rarer keys; and (iv) adaptive stratified sampling avoids or reduces key loss and leads to more consistent error bounds across keys.

In summary, our contributions include: (i) to our knowledge, our work is the first to apply multi-stage sampling theories to support sampling before arbitrarily long sequences of transformations while allowing estimated aggregate values to be computed with error bounds; (ii) we show how a data provenance graph can be constructed and combined with population estimation techniques to estimate quantities required by the

multi-stage sampling theories; (iii) we show how ASRS can be combined with multi-stage sampling for some applications to reduce key loss and equalize error bounds across popular and rare keys; (iv) we explore extensively the tradeoffs between sampling rates, execution time, key loss, and error bounds; and (v) we present an algorithm for automatically choosing sampling rates, and show that the algorithm can successfully choose sampling rates to meet user specified constraints on the CDF of error bounds for output values.

II. BACKGROUND AND RELATED WORK

Spark. Spark has emerged as a popular distributed data processing engine. Essentially, Spark extends and generalizes MapReduce programming model with its main data abstraction *resilient distributed datasets* (RDDs), which are fault-tolerant collections of data partitioned across a server cluster that can be processed in parallel [5]. RDDs can also be cached in memory for faster processing when reused. Spark includes two types of operations over an RDD, transformation and action. Transformations are lazy operations on an RDD that generate new RDD, whereas an action computes non-RDD values by triggering the RDD transformations. The computation results can either be stored in memory and returned to the driver program or written to disk.

Sampling in Spark. Applications amenable to approximation can improve their efficiency by leveraging the sampling mechanism provided by Spark. Unfortunately, it has several limitations which might hinder both efficiency and quality of approximation. *First*, applications usually need to load a large amount of data from external storage before a sequence of transformations on the input data. Spark only supports sampling on existing RDDs, which cannot reduce I/O time. *Second*, Spark sampling mechanism does not provide the error bound of computation results, which is very important for users to appropriately trade accuracy for saving computation time. *Third*, stratified sampling in Spark might still lose some keys, because it needs user to explicitly set sampling rates for each key and adopts Bernoulli Sampling to make a pass over all data items.

Approximate query processing. A variety of approximation techniques have been employed by query processing systems for execution time reduction. These techniques include using simple random or stratified sampling to construct samples to provide bounded errors [14]–[16] or online aggregation to sample data and produce a result within a time bound [17], [18]. BlinkDB [2] maintains a set of stratified samples by using an error-latency profile obtained by analyzing past queries. Sapprox [19] takes into account the storage distribution of the dataset for approximation. It collects the occurrences of sub-datasets in offline preprocessing and uses it to facilitate online sampling.

Online sampling. ApproxHadoop [20] introduces approximation to the MapReduce [21] paradigm. It performs cluster sampling over map tasks and data items within the chosen map tasks, which trades off result accuracy for execution

time reduction. Users can specify map task and data item sampling rates, ApproxHadoop then computes an estimated result with error bound. MaRSOS [16] implements stratified sampling [12] to address ApproxHadoop’s missing key issue. It minimizes oversampling on popular keys by leveraging a feedback system where mappers coordinate to sample. StreamApprox [22] is an approximation system based on Spark Streaming [23], targeting stream processing workloads. It also uses stratified sampling, so that the final sample has a representative sub-sample from each sub-stream (strata).

BlinkDB and Sapprox have an offline preprocessing component and assume data will be repeatedly used, whereas our work is an online approximation framework without the requirement of preprocessing the data. ApproxHadoop does not take the possible different semantics of the `Map` into consideration for computing the error bounds, e.g., `Map` operation can generate multiple data items in potentially different key spaces, which brings two challenges in the final error bound estimation- one is that the data items coming from the same parent data item essentially forms a new level of sampling cluster, another is that the population size of each new cluster would have to be estimated because for a data item that is dropped in the previous stage, whether it would generate a data item in some key space is unknown. ApproxHadoop does not differentiate between data items resulting from a `Map` that actually belong to different clusters, and simplifies the population estimation issue by homogenizing population sizes of different keys by assuming nonexistent data items to have values of zero [20].

ApproxSpark not only generalizes ApproxHadoop’s MapReduce paradigm to multi-step RDD transformations, it also addresses the aforementioned challenges by incorporating the clustering information and population estimation into the error bound computation. We also implement stratified sampling based on ASRS to address the key missing and unbalanced error bounds issue in ApproxHadoop. Compared to MaRSOS, ApproxSpark’s implementation of ASRS does not require coordination among parallel tasks, thus having less overhead and are still able to balance error bounds between popular and rare keys. We demonstrate ApproxSpark’s stratified sampling’s ability of balancing error between popular and rare keys empirically in the evaluation.

III. SAMPLING WITH ERROR BOUNDS

Consider a simple Spark program that loads a set of values (input data) into an RDD and sums them. We can reduce the I/O and work required for this computation by estimating the sum using a sample of the input data. Specifically, assuming that the input data spans multiple partitions, we create a sample by randomly choosing a subset of the partitions, and then randomly choosing a subset of input data items from each chosen partition. Given such a sample, we use a set of cluster sampling theories to estimate the sum ($\hat{\tau}$) and its variance (\hat{V}) [12]:

$$\hat{\tau} = \frac{N}{n} \sum_{i=1}^n \left(\frac{M_i}{m_i} \sum_{j=1}^{m_i} v_{ij} \right) \quad (1)$$

$$\hat{V}(\hat{\tau}) = N(N-n) \frac{S_u^2}{n} + \frac{N}{n} \sum_{i=1}^n M_i (M_i - m_i) \frac{S_i^2}{m_i} \quad (2)$$

where N is the total number of partitions (clusters), n is the number of partitions in the sample, M_i is the total number of data items (values) in partition i , m_i is the number of values from partition i in the sample, v_{ij} is the j^{th} value from partition i in the sample, S_i^2 is the sample intra-cluster variance for partition i , and S_u^2 is the sample inter-cluster variance. Note that N and M_i ’s are attributes of the input data set (population), while n and m_i ’s are attributes of the sample.

Now consider a slightly more complicated Spark program that loads input data into an RDD R_1 , applies a `map` to produce a second RDD R_2 , and then sums the values in R_2 . In this case, we can still sample when creating R_1 while using Equations 1 and 2 to compute the estimated sum and variance for values in R_2 . This is because `map` is a one-to-one mapping of items in R_1 to those in R_2 ; i.e., it transforms each item in R_1 into a single value in R_2 . Thus, performing the `map` on a sample of R_1 produces a sample of R_2 , with N and M_i ’s being the same for R_2 as for R_1 , and n and m_i ’s being the same for the sample of R_2 as for the sample of R_1 . In fact, we can sample at the beginning of an arbitrarily long sequence of transformations, as long as each transformation is a one-to-one mapping of items from its input RDD to its output RDD, and still use Equations 1 and 2 to compute the estimated sum and variance of the values in the final RDD. We simply map N and M_i ’s from the input RDD to the output RDD, and n and m_i ’s from the sample of the input RDD to the sample of the output RDD produced by the transformation chain.

A. Multi-stage sampling

Spark includes transformations that map input items to output items in more complex ways than one-to-one. For example, `flatMap` generates a group of output items for each input item, corresponding to a one-to-many mapping. In this case, choosing an item from the input RDD is equivalent to choosing a cluster of items from the output RDD, and choosing a cluster (partition) from the input is equivalent to choosing a cluster of clusters from the output. Sampling an input RDD in front of a sequence of transformations can thus correspond to multiple levels of cluster sampling (i.e., clusters of clusters of values) on the output RDD. This requires the use of multi-stage sampling theories, with potentially many stages (Equations 1 and 2 correspond to two-stage sampling).

The `filter` transformation, on the other hand, can produce zero output items for each input item, corresponding to a one-to-zero mapping. In this case, we cannot deduce the impact of clusters or items not chosen for the sample from the input RDD on the output RDD; i.e., some cluster/items not chosen from the input RDD would have produced items in

the output RDD, while others would not have. This introduces the need to estimate the population of the output RDD.

The above complications apply to many different transformations in multi-key computations. Consider a simple program to count word occurrences in a set of input sentences, where a `map` parses each sentence and produces a list of (word, 1) pairs, and a subsequent `flatMap` breaks the lists to produce an RDD of (word, 1) pairs. A `reduceByKey` is then used to sum the count of each unique word. It is straightforward to see that each input sentence will only contribute counts to a subset of the words and so the `map` is no longer a one-to-one mapping with respect to individual keys (words). Fortunately, multi-stage sampling and population estimation are sufficient to handle a set of common transformations for both single- and multi-key computations. We generalize the two-stage sampling theories shown in equations 1 and 2 to multiple stages for estimating sum and variance. Note that in a multi-key computation, a sample is chosen for each key, and we will need to estimate the sum and variance corresponding to each key.

Sum estimation. We estimate the sum $\hat{\tau}$ of a multi-stage sample with d sampling stages using the following recurrence:

$$\hat{\tau}_{I_k} = \begin{cases} \frac{N_{I_k}}{n_{I_k}} \sum_{j=1}^{n_{I_k}} \hat{\tau}_{I_k,j} & 0 \leq k < d, \\ v_{I_k} & k = d \end{cases}, \quad (3)$$

where $I_k = i_0, i_1, \dots, i_k$ is the index of a cluster at level k , $\hat{\tau}_{I_k}$ is the estimated sum of that cluster, N_{I_k} is the total number of sub-clusters, or if $k = d$, the total number of values in cluster I_k , n_{I_k} is the number of sub-clusters/values chosen from cluster I_k for the sample, $\hat{\tau}_{I_k,j}$ is the estimated sum of the sub-cluster j within cluster I_k , and v_{I_k} is the single value in cluster I_k in the last stage when $k = d$. The 0^{th} stage contains just one cluster comprising the entire population, and must always be chosen for the sample. $\hat{\tau}_0$ is then the overall estimated sum.

Variance estimation. According to the multi-stage sampling theory, estimating the variance involves computing the sum of inter and intra-cluster variance which are among and within the clusters. We can estimate variance using the recurrence:

$$\hat{V}(\hat{\tau}_{I_k}) = \begin{cases} \frac{N_{I_k}(N_{I_k} - n_{I_k})}{n_{I_k}} \frac{S_{u,I_k}^2}{n_{I_k}} \\ + \frac{N_{I_k}}{n_{I_k}} \sum_{j=1}^{n_{I_k}} \hat{V}(\hat{\tau}_{I_k,j}) & 0 \leq k < d, \\ M_{I_k}(M_{I_k} - m_{I_k}) \frac{S_{I_k}^2}{m_{I_k}} & k = d - 1 \end{cases}, \quad (4)$$

where $I_k = i_0, i_1, \dots, i_k$ is the index of a cluster at level k , $\hat{\tau}_{I_k}$ is the estimated sum of cluster I , S_{u,I_k}^2 is the sample inter-cluster variance at level k , and $S_{I_k}^2$ is the sample intra-cluster variance within each cluster I , $\hat{\tau}_{I_k,j}$ is the estimated sum of the sub-cluster j within cluster I_k . $\hat{V}(\hat{\tau}_0)$ is the overall estimated variance as the 0^{th} stage is an abstract stage represents the entire population.

Per-key population estimation. A Spark computation usually generates multiple keys, thus sampling before a transformation

is equivalent of sampling a mixed-key population where sub-population size of each key is unknown. However, the population size can be estimated from a sample size and sampling rate. We model estimated population size of a cluster as a negative binomial distribution parameterized by sample size and sampling rate i.e. $\hat{N}_{I_k} \sim \mathcal{NB}(n_{I_k}, p)$, where \hat{N}_{I_k} is the population size, n_{I_k} is the sample size and p is the level k cluster's sampling rate or the ratio of the data items that have passed through a filter. The intuition is that p , n_{I_k} and N_{I_k} corresponds to the success rate, number of successes and the number of trials in a binomial distribution. The unbiased estimator \hat{N}_{I_k} is simply $\frac{n_{I_k}}{p}$. The same logic also applies to the last sampling stage where the value of M_{I_k} needs to be estimated.

The uncertainty coupled with estimating N_{I_k} and M_{I_k} , must be included in computing the variances in equation 4 since their estimators affects the variance. We have detailed derivation on incorporating it into the variance computation in Appendix A.

Data provenance. Number of clusters or data items at each sampling stage has to be known in order to compute equations 3 and 4. To compute these parameters, we formulate a provenance graph covering the entire transformation chain that contains the mapping of input to output items by each transformation. The provenance graph allows the translation of sampling on the input RDD followed by the execution of a transformation sequence, to an equivalent multi-stage sample being taken from the final output RDD. Table I shows the subset of Spark transformations that our framework handles, and the provenance information that is kept. The provenance graph together with sampling rates also allow the estimation of population (i.e., number of sub-clusters or values) at each sampling level.

To form a provenance graph, information for computing the error is both logged "globally" at the driver program and "locally" at data items in the RDD. Information such as which RDDs have been sampled with their sampling rates, and RDDs that have been filtered is logged "globally" at the Spark driver program. The "global" information will be sent to the reducers when errors/cluster sizes are being estimated. Information that is logged "locally" is that, data items generated from the same parent data items by a `flatMap` will be tagged with the same id to indicate that they should be treated as next level clusters during the error computation process. The provenance graph needs to be walked backward to estimate cluster sizes in order to compute Equations 3 and 4.

Figure 2 shows an example provenance graph for a Spark sequence that samples the input data as it is read into RDD R_1 , which is then transformed by a `flatMap` into RDD R_2 . The driver program logs that cluster (partition) sampling and data item sampling took place when the input data file was read in to create RDD R_1 , and that there were a total of three blocks originally where one of them was dropped. The data items in R_2 are tagged to indicate clustering. This provenance graph is used to deduce that the input sampling and `flatMap`

| Transformation | Functionality | Provenance information |
|-----------------|--|---|
| map(func) | Applies func to each data item. | Number of data items for every output key for each input data item. |
| flatMap(func) | Applies func to each data item, then flattens the results. | Clustering of output data items produced from each input data item. |
| mapValues(func) | Applies func only to the value of each tuple. | Number of data items for every output key for each input data item. |
| filter(func) | Selects data items that satisfy a predicate (func). | Ratio of the data items that have been filtered out. |

TABLE I: Spark transformations that can be approximated by ApproxSpark, their functionalities, and the mapping of provenance information from input RDD to output RDD.

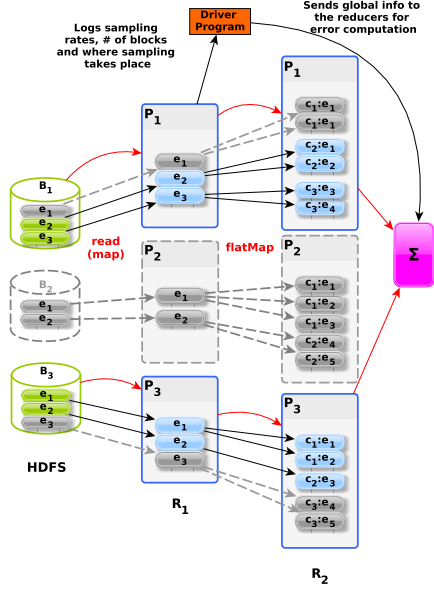


Fig. 2: Example showing HDFS blocks and data items being sampled when read into RDD R_1 . Block B_2 is dropped entirely, and data item e_1 in B_1 and e_3 in B_3 are dropped. In R_2 , $c_i : e_j$ means the j^{th} data item in a partition generated from the i^{th} data item in the corresponding input RDD partition. The nonexistent data items and blocks/partitions are in grey.

transformation is equivalent to a three-stage sampling on the "precise" RDD R_1 . Specifically, e_3 in block 3 is dropped when loading the file into R_1 , it would generate a small cluster in R_2 had it not been dropped. As a result, dropping e_3 corresponds to dropping a subcluster in partition 2 in RDD R_2 , where partitions are the primary sampling clusters. Equivalently, it can also be viewed as taking a three-stage cluster sample from RDD R_2 , partition P_2 is first dropped from the first-level clusters which are RDD partitions, and secondary clusters in P_1 and P_3 are dropped in the next stage where they are marked as c_1 and c_3 .

Confidence interval. We can define the confidence interval as $\hat{\tau}_0 \pm \epsilon$ where $\epsilon = t_{n-1, 1-\alpha/2} \sqrt{\hat{V}(\hat{\tau}_0)}$ [12], $t_{n-1, 1-\alpha/2}$ is the critical value under the Student's t distribution at the desired level of confidence α , and n is the degree of freedom (i.e., the number of partitions).

B. Stratified reservoir sampling

An inherent limitation of the above multi-stage sampling is that some rare keys in the output may be lost. Moreover, when rare keys do appear in the output, they are often accompanied with a large error bound.

We leverage an one-pass sampling algorithm *Adaptive Stratified Reservoir Sampling* (ASRS) [13] to address the rare key issues. ASRS combines stratified sampling [16], [24] and reservoir sampling [25], and uses power allocation [26] to divide the total sample size among different strata proportionally to each stratum's moving sampling error. ASRS dynamically increases the sampling rates of rare keys to compensate for their larger sampling errors and reduces oversampling the popular keys by decreasing their sampling rates. Details of reservoir size allocation algorithm can be found in [13].

Integration with partition sampling. The downside of pure ASRS is its larger overhead compared to simple random sampling. In order to achieve balance in the trade-offs among output key retaining, balanced error bound distributions and the overall execution time, we sample RDD partitions at the input and apply ASRS over the their elements, so that in the chosen RDD partitions, sampling errors among popular and rare keys are more even and rare keys are better retained. Partition sampling at the input will have significant execution time saving since much I/O time is reduced. We can still estimate the result and the error bound using standard multi-stage sampling theory, the reason is that the stratified sample obtained from [13] is very close to a simple random sample which suggests equations 3 and 4 can be used to estimate the error. However, a limitation of ASRS is that it needs to know the keys to apply sampling, thus ASRS cannot be placed before the keys are generated unless the mapping relationship of the final key and the keys that are directly balanced by ASRS is known.

IV. APPROXSPARK

We have implemented our approximation mechanisms by either modifying or extending the original Spark framework. For example, we extend `SparkContext`, the master of Spark application, to globally track which RDD sampling is applied to and the sampling rates, number of sampling stages, etc. We also extend Spark's `StatCounter` class to store intra and inter-cluster variances, sample sizes, sampling rates, etc. ApproxSpark offers two methods for user to set the degree

of approximation, either by specifying the sampling rates or error bound targets.

A. User-specified sampling rates

Multi-stage cluster sampling. We modify the partition loading and computation mechanisms in the `HadoopRDD` class to support partition/input data item sampling when data is being loaded into an RDD. Subsequent RDDs' data items can be sampled using the original `sample` transformation in Spark API.

In order to forward information to the output RDD as in Table I, we modify the implementations of those transformations in RDD class. For example, `flatMap` forwards the information that groups of data items generated from the same data item i in the input RDD by tagging them with a cluster id c_i .

The error bounds are computed in both the action and transformation phases. Each partition's running statistics in multi-level clusters, such as the estimated sums and variances, are computed recursively in the transformation phase locally within a Spark executor instance. Then the statistics of each partition is sent to the reducers via shuffling for further computation on the final confidence interval in the action phase. For efficiency purposes, we adopt an online algorithm [27] that computes variances of the data items incrementally on the fly.

ApproxSpark implements a new RDD transformation `aggregateByKeyMultiStage`, for both intra and inter partition aggregations when multistage sampling is used. It is similar to RDD's original `aggregateByKey` but has added error bound computation mechanisms.

Stratified reservoir sampling. We modify ASRS to be executed in Spark's distributed environment by dividing the total reservoir size, taken as a user input, evenly among RDD partitions. Each partition is sampled using ASRS independently without coordination among them.

We implement ASRS as a transformation that produces another RDD, containing the resulting sample with balanced sampling errors among popular and rare keys. ASRS changes the sampling rate by changing the size of the portion of the reservoir allocated for a particular key. On the other hand, ASRS shrinks the size allocated to each existing key as it discovers more keys in the partition, the initial reservoir size for the new key is set as the average of the sizes for existing keys. The benefit of implementing ASRS as a transformation is that the resulting RDD can be cached in memory for reuse.

We provide user `ASRSSample` to sample RDD using ASRS and `aggregateByKeyStratified` for the aggregation with error bound computation, both implemented as RDD transformations.

B. User-specified target error bounds

In addition to sample RDDs with specified sampling rates, user is also able to set target error bounds at different percentiles for the error bound CDF of all keys. For example, a user may specify that the 10th percentile of the error bound

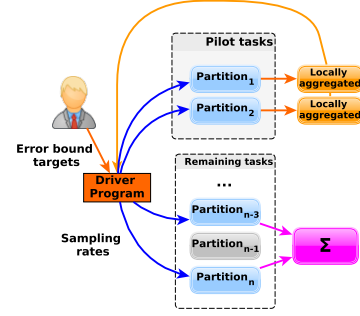


Fig. 3: User setting error bound targets design, gray shaded box is dropped partition(s).

is at most 0.1, the 50th percentile at 0.3, the 90th percentile at most 0.6. We have implemented a simple version handling two-stage sampling.

$pCluster = 1.0$;

$pItem = 1.0$;

input : Target error bounds at n percentiles, $t_{perc1}, t_{perc2} \dots t_{percn}$ ($t_{perc1} \leq t_{perc2} \leq \dots \leq t_{percn}$), search step sizes for cluster and item sampling rates, $bstep$ and $dstep$

output: $pCluster$ and $pItem$

—————Phase

I

Execute pilot tasks and return partially aggregated partitions to the driver;

For each key, in the driver program:

Estimate M , the number of data items in each partition;

Estimate S_u^2 , the inter-cluster variance;

Estimate S_i^2 , the intra-cluster variance in each partition;

—————Phase

II

while None of the predicted percentile points exceeds the target error bounds **do**

 Use $pCluster$ to compute error bounds in $perc1, perc2 \dots percn$;
 $pCluster -= bstep$;

end

$pCluster += bstep$;

while None of the predicted percentile points exceeds the target error bounds **do**

 Use $pCluster$ and $pItem$ to compute error bounds in $perc1, perc2 \dots percn$;
 $pItem -= dstep$;

end

$pItem += dstep$;

Continue the remaining Spark tasks setting sampling rates to be $pCluster$ and $pItem$;

Algorithm 1: Two-stage sampling rates search algorithm

We propose a greedy algorithm to search for a sampling rate combination leading to a potentially tightest error bound distribution constrained by the target errors, while aiming to reduce execution time to the greatest extent. Initially, partition

and data item sampling rates (pCluster and pItem) are both initialized as 1.0, i.e. no sampling. The algorithm includes two phases, where it respectively estimates necessary statistics to predict error bounds and searches for the sampling rates. In the first phase, a wave of pilot tasks are executed and the partially aggregated results from these tasks are sent back to the driver program, where the number of data items M and inter/intra cluster variances for each key are computed. It uses a Spark’s job submission mode that returns the partially aggregated partitions to the driver instead of sending them for shuffling. In the second phase, the algorithm uses statistics gathered in the first phase to predict error bounds: it first lowers partition sampling rate for potentially maximum execution time reduction until it would violate an error bound target, then it searches for an appropriate input data item sampling rate, also until the predicted error CDF would violate any of the user-specified targets. When predicting errors for keys that are not encountered in the first phase, the algorithm just uses the average of the statistics for the keys that are seen in the first phase. Lowering the data item sampling rates makes the CDF curve shift right at a finer granularity. When the predicted error distribution meets all the error targets with the lowest possible sampling rates, the algorithm stops and uses them for the remaining Spark tasks. Figure 3 shows the system design of user-specified error bounds.

The greedy heuristic leverages a fact that partition sampling incurs more sampling errors than data item sampling [12], but reduces more execution time. Our algorithm follows a principle in online aggregation- *minimum time to accuracy* [17], i.e. minimizing the time to achieve a useful estimated value. However, online aggregation typically outputs a running confidence interval for an estimator as data is being aggregated in a random order, whereas ApproxSpark applies multi-stage sampling over the data and outputs the error bounds for all keys at the end of execution.

Limitations. A limitation of the algorithm is that it assumes the keys are distributed evenly among partitions, so that the pilot partitions are representative with regards to the entire dataset. When keys are not distributed evenly across the partitions or only exist in a few, the pilot wave is not able to estimate the parameters accurately. The error bound computation in our implementation has only considered two-stage sampling, we did not implement the case when there are filters in the transformations that would involve population estimation. We leave this more complicated case as future work.

V. EVALUATION

We evaluate ApproxSpark using five real world applications from different application domains (see Table II). We begin by briefly describing the applications. We then use them to extensively explore the tradeoff space between sampling and precision. Finally, we briefly explore ApproxSpark’s ability to find appropriate sampling rates for user specified target error bound constraints.

| Application | Domain | Input Data Set | Size (GB) |
|-------------|----------------|-----------------------|-----------|
| Co-occur | Text Mining | MEDLINE database | 7.5 |
| Speed | Smart City | GPS trace | 36.0 |
| Twitter | NLP | Tweets2011 (TREC) | 2.2 |
| PageRank | Graph Analysis | Wikipedia snapshot | 53.0 |
| Clickstream | Log Analysis | Wikipedia clickstream | 6.5 |

TABLE II: List of applications, the domains they come from, and the input data sets used in our evaluation.

Experimental environment. All experiments are run on a cluster of four servers. Each server is equipped with a 2.5GHZ Intel Xeon CPU with 12 cores, 2 hyperthreads per core, 256GB of RAM, and a SATA hard disk. The cluster is interconnected with 1Gbps Ethernet. All servers run Linux 3.10.0. ApproxSpark extends Spark version 1.6.1 and is configured with 16 executors, each of which runs up to 6 tasks, so that each server has 4 executors, running up to 24 tasks.

A. Applications

Word Co-occurrence (Co-occur). This application computes the co-occurrence frequencies of pairs of words. Word co-occurrence analysis is a common method used in many text mining applications [28]. In this study, the application counts co-occurrences of topic tags in the MEDLINE database [29], containing more than 20M citation records of publications in life sciences and medicine. Each citation record contains a set of topic tags, listing the major topics relevant to the publication. The task is to count the total frequencies of co-occurring tag pairs.

The application first reads the input data into an RDD, and then performs a `map` to extract the list of major topic tags from each citation record. It then performs a `flatMap` to generate key-value pairs ((co-occurring tag pair), 1). Finally, it sums and outputs the count of each co-occurring tag pairs.

Vehicular Average Speed Analysis (Speed). This application analyzes the average speed of vehicles moving in a geographical area each hour at three different granularities: around a point-of-interest (POI) (e.g., a restaurant), on a road segment, and within a region. An analysis of vehicular traces is useful for monitoring urban traffic, predicting passenger demand, recommending taxi routes, etc. [30], [31]. We analyze a taxi GPS dataset containing status records collected every 30 seconds from 14,000 taxis operating in Shenzhen, China over one week [31]. Each record contains information about a taxi, including a timestamp and the taxi’s GPS location and speed. The dataset has ~ 291 M records that covers an area of ~ 790 square miles divided into 491 regions, containing ~ 569 k POIs and ~ 198 k road segments. Each POI is assigned to a road segment and each road segment belongs to a region.

The application reads the input data into an RDD, and then performs three transformations and three actions. The three transformations are three `map` operations that: (1) transform each GPS entry into a ((POI, hour), speed) key-value pair; (2) transform each ((POI, hour), speed) pair into a ((road segment, hour), speed) key-value pair; and, (3) transform each ((road segment, hour), speed) pair into a ((region, hour), speed) pair.

The three actions use the three intermediate RDDs to compute the average speed per hour at each POI, each road segment, and each region, respectively.

Twitter Hashtags Sentiment Analysis (Twitter). Sentiment analysis computes quantitatively whether a piece of text is positive, negative or neutral using natural language processing (NLP) techniques. It is often used to gauge opinions toward entities such as products, services, events, etc. It has wide applications in many different fields, such as marketing, politics, and customer service [32]. In this study, the application computes the average sentiment for each unique hashtag in the Tweets2011 Twitter dataset from TREC 2011 [33], using the Stanford CoreNLP library [34]. This dataset contains $\sim 16\text{M}$ tweets sampled over 17 days in early 2011.

The application first reads the input data into an RDD, and then performs a `map` to compute a sentiment score in the interval $[0, 6]$ with 0 being *very negative*, 3 being *neutral*, and 5 being *very positive* for each tweet. It then performs a `flatMap` to extract all hashtags from each tweet and associates each with the sentiment score for the tweet. Finally, it computes and outputs the average sentiment for each hashtag.

WikiPageRank (PageRank). This application counts the number of articles that link to each article in a set [35], emulating one of the main processing components of PageRank [36]. We use the Wikipedia data snapshot from 2016 with $\sim 5\text{M}$ articles [37]. The application first loads the data into an RDD, then applies a `map` to parse the XML, generating a list of outbound links for each article. It next performs a `flatMap` to generate pairs of (destination article, 1). Finally, it sums and outputs the count for each destination article.

WikiClickstream (Clickstream). Clickstream analysis can be used to generate a weighted network of linked articles showing the probability of users navigating from one article to another. We use a Wikipedia clickstream dataset from 2016 [38] containing $\sim 149\text{M}$ tuples of (source, destination, count), where count is the number of times that a user has visited the destination page from the source page. The application computes the total count for each unique (source, destination) pair. Specifically, it reads the input data into an RDD, performs a `map` to generate a key-value pair for each entry, and then sums and outputs the total count for each unique (source, destination) pair.

B. Results for multi-stage sampling

We explore the performance and accuracy of multi-stage sampling using four of the above applications: Co-occurrence, Twitter, WikiPageRank, and WikiClickstream. In most experiments, we sample the input data as it is read into the first RDD because this will lead to the highest speedups. However, we also explore sampling from RDDs later in the applications' transformation chains to explore the trade-off between performance and accuracy of such scenarios.

Execution times. Figure 4 plots the execution times for three of the applications, Co-occurrence, WikiPageRank, Wi-

kiClickstream at different partition and data item sampling rates. Consistent with previous results from [20], we observe that (a) multi-stage sampling significantly reduces execution times, and (b) partition sampling can lead to larger execution time savings than data item sampling. This latter is because dropping a partition eliminates overheads such as I/O time for reading the blocks, the creation of an RDD partition in memory, etc., whereas data item sampling still requires some processing for each partition. The sampling framework imposes some overheads; i.e., execution time for the (100% (partition sampling), 100% (data item sampling)) case is somewhat greater than that of the precise version.

Fraction of keys in output. As already mentioned, multi-stage sampling can result in loss of keys in the output for jobs that produce more than one key. Figure 5 plots the fractions of keys present in the output at different sampling rates for the same three applications, normalized against the total number of keys produced in the precise executions. Figure 6 shows the occurrence frequencies of lost keys in the input RDD of the final aggregation action in a precise execution, normalized against the total number of data items in the RDD.

We observe that significant fractions of keys can be lost, especially at higher partitioning sampling rates. For example, sampling rates of (75%, 60%) for Co-occurrence reduce execution time by 40% at the expense of losing 25% of the keys produced by the precise execution. However, Figure 6 shows that only *rare* keys are lost. For example, for the same (75%, 60%) sampling rates in Co-occurrence, the most frequently appearing key that was lost accounted for only a very small fraction 0.85×10^{-4} of the total number of data items in the input RDD of the final aggregation action, while 90% of the lost keys each accounted for less than or equal to 0.08×10^{-4} of the total number of data items in the RDD. The lost keys are even more rare in the WikiPageRank and WikiClickstream applications, where the occurrences of each lost key accounting for 10^{-7} of the total number of data items.

Effect of sampling rates on error bounds. Figure 7 plots the CDFs of the relative error bounds, which are the ratios of sampling error to estimated value, for all keys with 95% confidence for Co-occurrence. Each graph in the figure plots CDFs for several different partition sampling rates and a single data item sampling rate, with different graphs having different data item sampling rates. We observe that, as pointed out in [16], multi-stage sampling without considering keys in the final output over-samples popular keys and under-samples rare keys, leading to uneven relative error bounds. This can lead to large relative error bounds in the tails of the relative error bounds CDFs.

We observe that even relatively high partition sampling rates (e.g., 75% - green curve in Figure 7(a)) can significantly impact error bounds for more rare keys (pushing the CDF curve for $>60\%$ to the right) while not affecting the frequently appearing keys much (the CDF curve does not change much for $<60\%$). Interestingly, a 75% partition sampling rate affects error bounds less or comparable to a 75% data item sampling

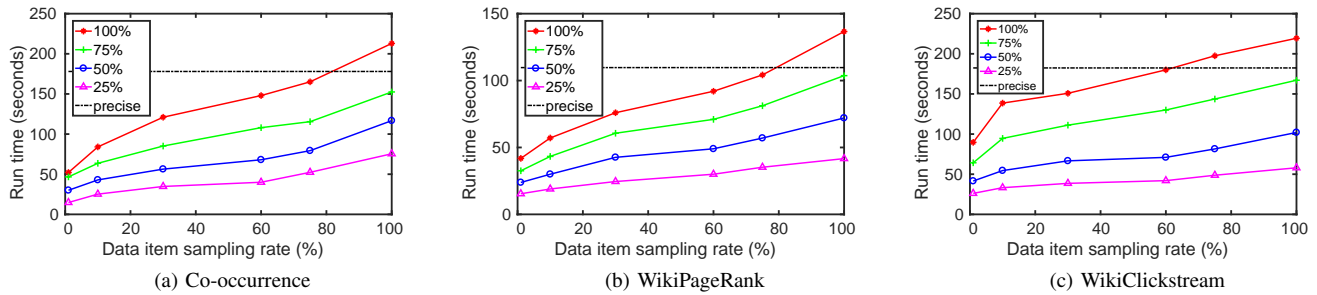


Fig. 4: Execution times under different sampling rates. Multi-stage sampling is performed when the input data is read into the first RDD. Each line corresponds to a different partition sampling rate. The x-axis shows the sampling rate for selecting data items within each chosen partition. The dashed horizontal line gives the runtime of the precise version of the application. Each point is the average execution time of 20 runs.

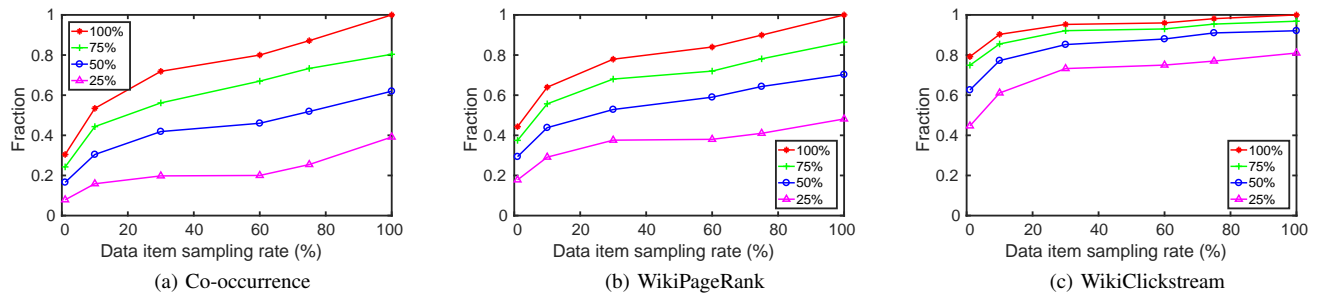


Fig. 5: Fraction of unique keys (normalized against number of keys produced under precise execution) outputted under different sampling rates. Each line plots the fractions of keys in the output at a particular partition sampling rate.

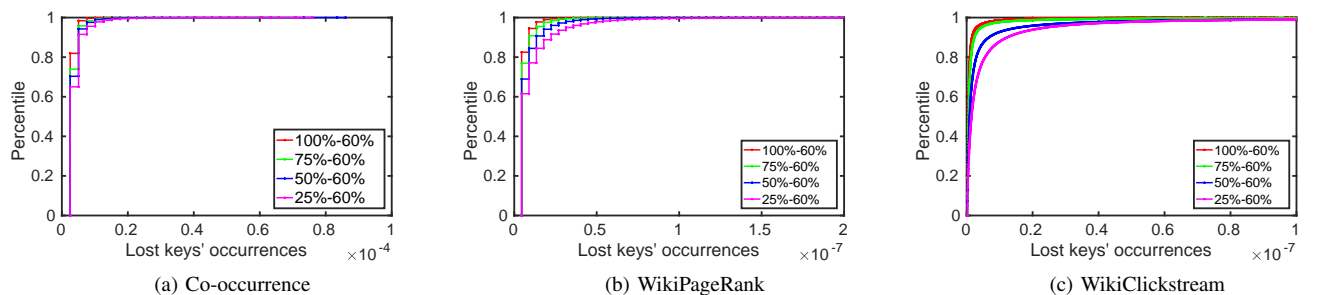


Fig. 6: CDFs of occurrences of the lost keys, normalized against the total number of data items across all keys at a data item sampling rate of 60%. Each line corresponds to a specific partition sampling rate.

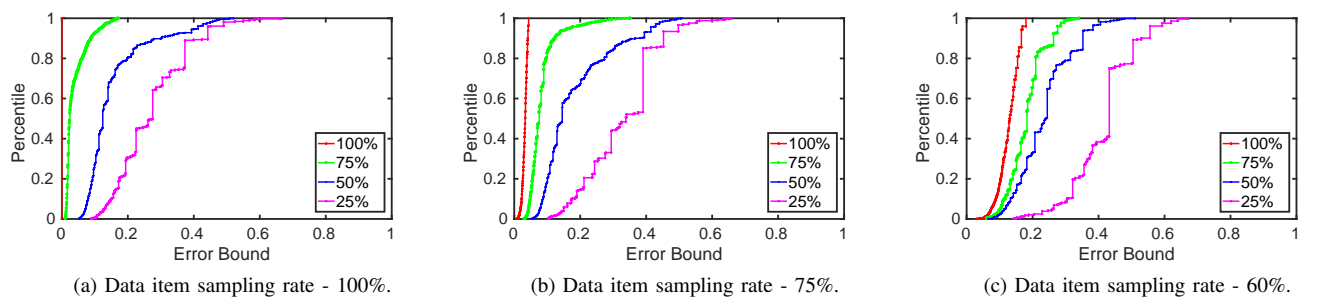


Fig. 7: Each graph plots CDFs of errors with 95% confidence error at a fixed input data item sampling rate for Co-occurrence application. Each line in a graph plots the error CDF at a particular partition sampling rate.

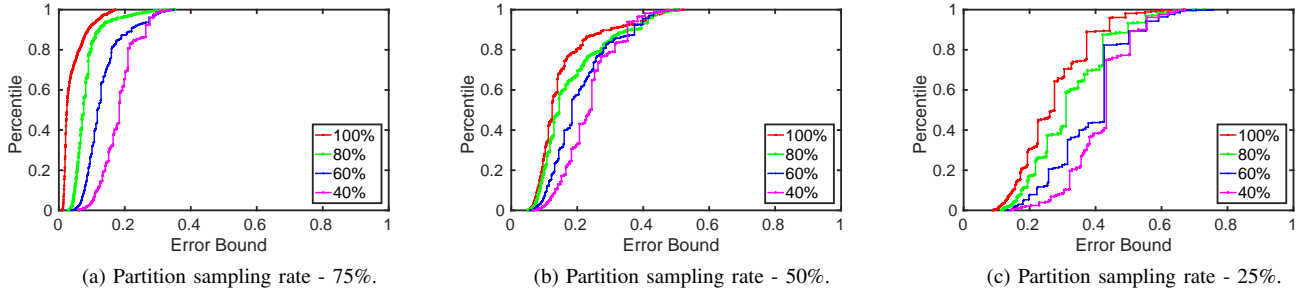


Fig. 8: CDFs of errors with 95% confidence error at a fixed partition sampling rate for Co-occurrence application. Each line in a graph plots the error CDF at a particular input data item sampling rate.

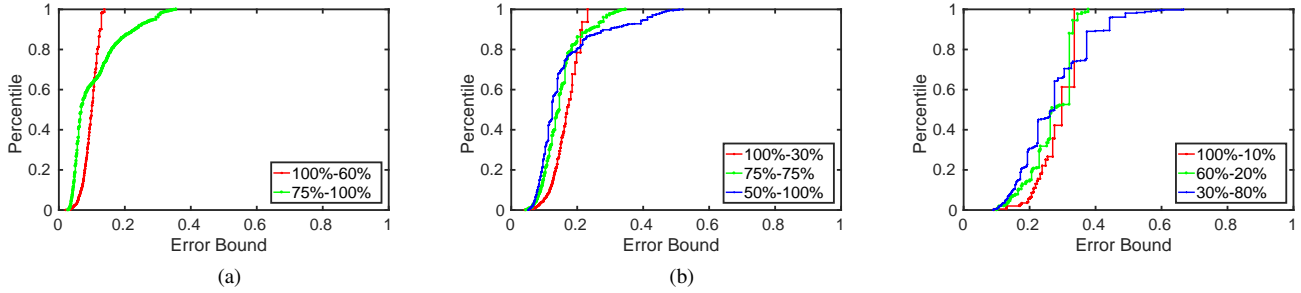


Fig. 9: Error distribution trade off under different partition and data item sampling rates combination from the Co-occurrence application. The legends indicate partition and data item sampling rates respectively.

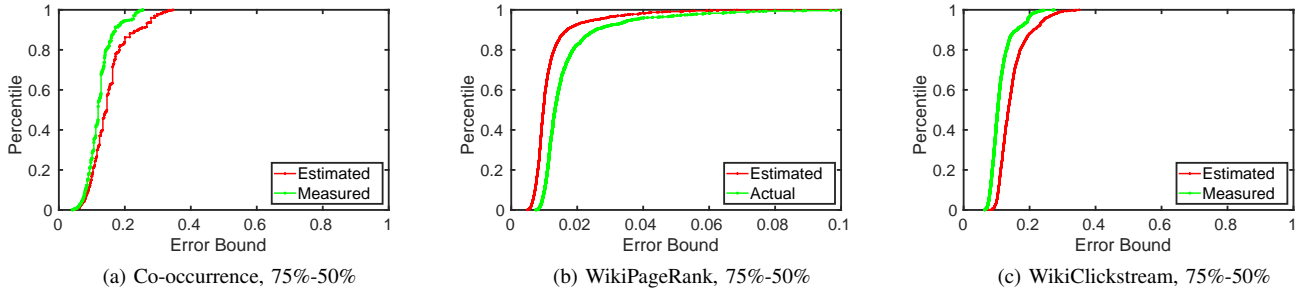


Fig. 10: Estimated error bounds and actual relative error comparison.

rate (red curve in Figure 7(b)) for up to 60% of the keys, but the tail is significantly worse for partition sampling. We believe this is caused by the clustering of data items with the same keys within partitions. As either or both sampling rates decrease, the entire error bound CDF shifts to the right (larger error bounds). However, the observation that partition sampling affects the tail of error bounds CDF much more strongly than data item sampling remains consistent throughout.

Figure 8 shows the error bound CDFs when the partition sampling rates are fixed with varying data item sampling rates, the tails of the error bound CDFs are similar under the same partition sampling rates. This points to a fundamental trade-off: partition sampling can reduce execution time over data item sampling, but trades off higher error bounds for the rarer keys to do so.

Figure 9 shows that the 95% relative error CDFs can exhibit trade-offs with different combinations of partition and data item sampling rates. In each subgraph, the sampling rates are chosen so that they have similar execution time as in Figure

4(a). We can see that their error CDFs intersect, with the error CDFs from lower partition sampling rates having worse tails. It shows that different partition and data item sampling rates combinations can achieve similar execution time, but different error bound distributions. For example in Figure 9(a), (100%-60%) has better smaller errors after the 62th percentile, but performs worse on frequent keys that have smaller errors. It is because (100%-75%) processes more data than (100%-60%), so the frequent keys result in smaller errors but the rarer keys have worse error due to partition dropping. Figure 10 plots the distributions of estimated error bounds obtained through the multi-stage sampling theory, against the actual relative error computed using the ground truth: $\epsilon = |1 - \frac{\hat{v}}{v}|$. We can see that ApproxSpark’s error estimation is more accurate at lower percentiles and less so at higher percentiles. It is because the popular keys usually have smaller error bounds which provides more statistical information to the error estimation process and vice versa.

| Source | Sampling Rates | |
|--------------------------|----------------|------------|
| | (100%, 30%) | (75%, 75%) |
| Partition sampling | 0% | 78% |
| Data item sampling | 88% | 12% |
| Pop. estimate partitions | 0% | 5% |
| Pop. estimate data items | 12% | 5% |

TABLE III: Breakdown of uncertainty on average across all keys for the four sources of errors in multi-stage sampling for Co-occurrence.

| Sampling Rates | Execution Time (s) | Error Bound 100 th | 90 th | 50 th | % Keys Present |
|----------------|--------------------|-------------------------------|------------------|------------------|----------------|
| 100%-60% | 149.2 | 0.17 | 0.12 | 0.10 | 80.0 |
| 75%-100% | 150.8 | 0.37 | 0.22 | 0.06 | 80.3 |
| 100%-30% | 120.9 | 0.22 | 0.20 | 0.17 | 71.8 |
| 75%-75% | 121.4 | 0.32 | 0.28 | 0.13 | 72.3 |
| 50%-100% | 119.7 | 0.51 | 0.31 | 0.11 | 61.5 |

TABLE IV: Comparison of run times, error bounds CDF at 100th, 90th, 50th percentiles, and fraction of unique keys for Co-occurrence application.

Sources of uncertainty. As previously explained, uncertainties (leading to estimated error bounds) can arise from the sampling as well as population estimations. Table III shows the percentages of the error bounds, averaged across all keys in the output, attributable to each of four sources for Co-occurrence. We observe that the inter-cluster variance from partition sampling accounts for by far the largest portion of the estimated error bounds, which is consistent with [12]. The intra-cluster variance from data item sampling accounts for the next largest portion, while population estimations for number of partitions, the number of groups of co-occurred words, within each partition for each key, account for only small portions of the error bounds.

Sensitivity to underlying data distribution. In the dataset for our Twitter application, the tweets are ordered chronologically which implies that the keys (Hashtag) tend to cluster. We explored shuffling the data items and see what effects it has over the result.

Sampling error. Sampling error is smaller in the shuffled data case. It because when data items is shuffled, there is less inter-cluster variance and less uncertainty in population size estimation. Figure 13 shows the comparison of sampling error CDFs between the shuffled and unshuffled data when applying a 50% partition sampling rate.

Fraction of keys shown in the output. Effect of sampling partitions misses fewer keys when the input data is shuffled, mitigating the clustering effect of the keys. So if temporal info is not important to the application, shuffling the data offline as preprocessing will improve the result in terms of sampling error and number of missed keys, assuming data will be reused.

Summary. Putting together the observations made above, we conclude that multi-stage sampling works well to sig-

nificantly reduce execution time while introducing small to modest relative errors, as long as the loss of rare keys are acceptable. Further, data item sampling would typically be preferable to partition sampling because it gives more consistent error bounds across keys. To more clearly support this conclusion, Table IV presents data for two sets of sampling rates for Co-occurrence, $\{(100\%, 60\%), (75\%, 100\%)\}$ and $\{(100\%, 30\%), (75\%, 75\%), (50\%, 100\%)\}$, where members within each set have similar execution times. As the partition sampling rate increases, the tail of the error bounds CDF worsen significantly. The trend is less clear for lost keys; however, high partition sampling rates (e.g., 50%) can clearly lead to significantly increased number of lost keys. Looking at Figure 4 (a), this implies that partition sampling rates of 50% and 75% are not as useful since similar performance is achievable with (100%, $x\%$) sampling rates. On the other hand, execution time can be reduced using a partition sampling rate of 25% if one is willing to tolerate the accompanying key loss and increased error bounds.

C. Results for stratified reservoir sampling

In the Speed application, we explored both stratified reservoir and simple random sampling on the data items in POI RDD, together with the RDD partition dropping when reading the input data. Either stratified/simple random sampling is performed over the data items in the POI RDD, providing stratification effect for both road segment and region RDDs. We also use power allocation techniques to balance the sampling errors at each strata in the POI RDD.

Execution times. Figure 11 shows that aggregating the street and region RDD both has run time reduction as the sampling rate on the POI RDD lowers, whether stratified or simple random sampling is performed. Stratified reservoir sampling has higher execution time than the simple random sampling method since it needs to perform stratification and power allocation.

Confidence interval. Figure 12 plots the estimated values with error bars of the average speed at the region level. The precise result is plotted in the dashed black curves, estimated value in green curve and 95 % confidence intervals as red error bars. Usually higher average speed is observed in regions that are away from city centers and at hours that are early in the morning or late night, as a result these points come with lower taxi densities, i.e., fewer samples which also tend to cluster over a few partitions. These points would have larger error bars without balancing the sample sizes among popular and rare keys, as shown in the Figure 12 (a) and (c), whereas stratified reservoir sampling coupled with power allocation technique increases the sampling rates of these rare keys, which result in smaller error bars. However, the popular keys have shorter error bars under simple random sampling technique compared to stratified sampling as a result of power allocation.

Fraction of keys shown in the output. In Figure 14 (a), we see that the output loses more keys as the RDD partition and data item sampling rates lower under simple random sampling

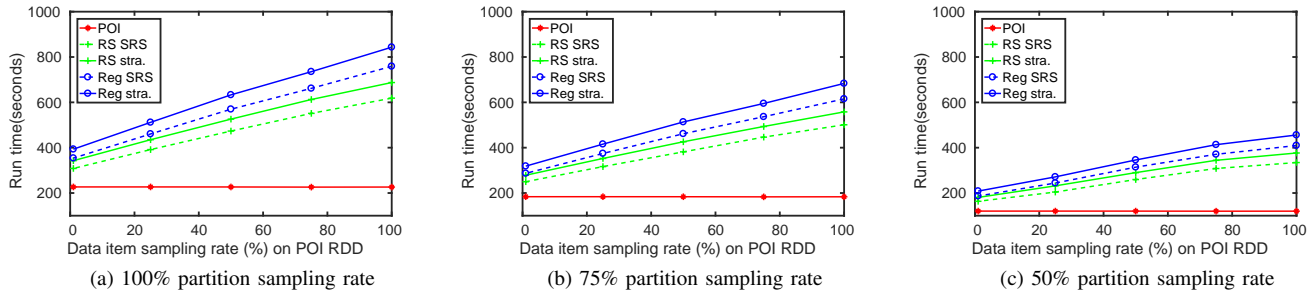


Fig. 11: Run times for the aggregations at POI, road segment and region RDD. The dashed curves represent the aggregation run times under simple random sampling whereas the solid curves represent the run times under stratified sampling. RS SRS - Road segment simple random sampling, RS stra - Road segment stratified sampling, Reg SRS - Region simple random sampling, Reg stra - Region stratified sampling.

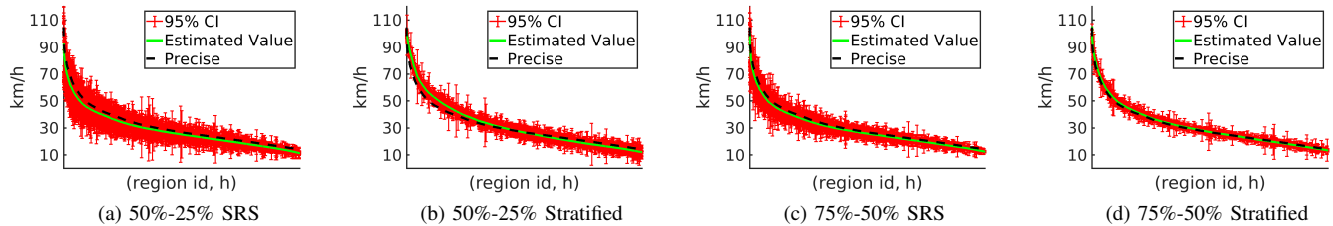


Fig. 12: Region average speed at each hour. Comparisons of 95 % Confidence Interval when sample random sampling and stratified reservoir sampling is applied at the POI level RDD, coupled with partition dropping at the input GPS trace. The first rate is the partition sampling rate, the second is the sampling rate used at the POI RDD.

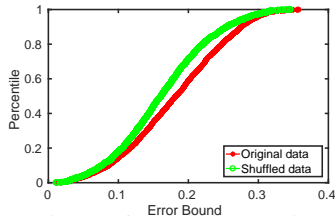


Fig. 13: Comparison of error bound in twitter application between the shuffled data and unshuffled data when applying 50% partition sampling rate.

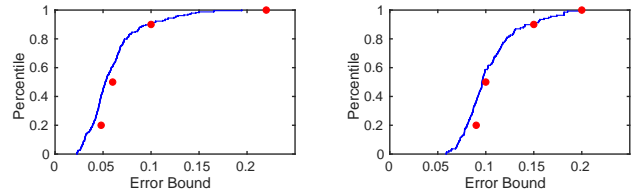


Fig. 15: User setting error bounds targets on the CDF.

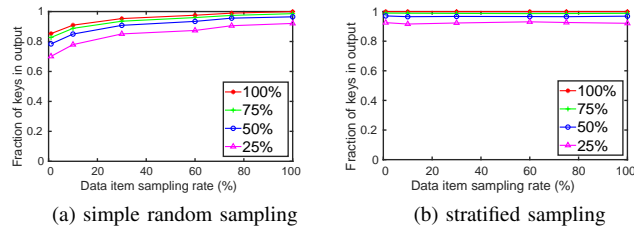


Fig. 14: Number of keys (normalized) for aggregation at road segment level, simple random sampling or stratified sampling performed at the road segment RDD. Each line represents a partition sampling rate at the GPS RDD.

at POI RDD, the number of keys grows faster than linear as data item sampling rate increases. In Figure 14 (b), we see that stratified sampling almost preserves the number of keys (with some fluctuation due to randomization effect from sampling) under the same partition sampling rate. This shows

that stratified reservoir sampling is much better at preserving keys in the result whether partition sampling is applied.

D. Results for user-specified error targets

We now demonstrate ApproxSpark’s capability in allowing users to set error bounds target at different percentiles over the relative error distribution. The red dots in Figure 15 show the target error bounds at 20th, 50th, 90th, 100th percentiles; the blue curves show the resulting CDF achieved by ApproxSpark, setting both partition and data item sampling step sizes to be 0.1%. We can see that the CDFs are bounded by the targets set by the user. Figure 15 (a) is the error distribution for average Taxi speed with 50% partition sampling rate and 80% data item sampling rate at the POI RDD. Figure 15 (b) is the error distribution for Wikiclickstream aggregation result with only 50% input data item sampling rate and 60% partition sampling.

E. Summary for evaluation

Lots of trade-off options when choosing sampling rates, sampling technique, where to sample. For example, sampling partitions saves the most run time but may increase the error bounds, stratified sampling with power allocation makes the error bound more evenly distributed among different keys, loses fewer keys but incurs more execution overhead. We also have found that input data that contains less rare keys for the application is more amenable to approximation since fewer keys are missed and error bound overall is smaller.

VI. CONCLUSION

In this paper, we motivate, design, and implement a system called ApproxSpark. ApproxSpark features a set of approximation mechanisms leveraging sampling theories to adapt to Spark's computing paradigm with multi-step RDD transformations. We demonstrated how error bounds are estimated in case of multiple transformations. We utilize a set of metrics to rigorously evaluate ApproxSpark including run times, the error bound distribution for all keys, number of keys missed, and error bars, using applications from different domains. We also demonstrated that there is an interesting yet complicated trade-off space in terms of the error bounds, run times and number of keys, when choosing different sampling schemes, such as specific sampling rates, partition vs data item sampling, whether to use stratified or simple random sampling etc. Different combinations of partition/data item sampling rates achieves different error bound distributions while maintaining similar run times. In a real-world setting, a user would choose the most appropriate sampling setup catering to her approximation goal. Based on our experience and results, we conclude that our framework and system can make efficient and customized approximation to Spark users.

APPENDIX

Estimated sum for all clusters is:

$$\hat{\tau} = \frac{\hat{N}}{n} \sum_{i \in S} v_i = \hat{N} \bar{\tau} \quad (5)$$

Sample mean among the cluster totals is:

$$\bar{\tau} = \frac{1}{n} \sum_{i \in S} v_i \quad (6)$$

Estimated total number of clusters N is:

$$\hat{N} = \frac{n}{p_1} \quad (7)$$

Since $\hat{N} \sim \mathcal{NB}(n, p_1)$, the variance of \hat{N} is:

$$\text{Var}(\hat{N}) = \frac{n(1-p_1)}{p_1^2} \quad (8)$$

If we treat it as simple random sampling, the variance of mean of cluster total is:

$$\text{Var}(\bar{\tau}) = (1-p_1) \frac{s_t^2}{n} \quad (9)$$

Variance of cluster totals $\text{Var}(\hat{\tau})_{srs} =$

$$\begin{aligned} & \text{Var}(\hat{N}\bar{\tau}) \\ &= \hat{N}^2 \text{Var}(\bar{\tau}) + \bar{\tau}^2 \text{Var}(\hat{N}) + \text{Var}(\hat{N})\text{Var}(\bar{\tau}) \\ &= \left(\frac{n}{p_1}\right)^2 (1-p_1) \frac{s_t^2}{n} + \frac{n(1-p_1)}{p_1^2} (\bar{\tau}^2 + (1-p_1) \frac{s_t^2}{n}) \end{aligned} \quad (10)$$

thus:

$$\text{Var}_{inter} = \left(1 - \frac{1}{p_1}\right) \text{Var}_{srs}(\hat{\tau}) \quad (11)$$

Estimated sum of cluster i is:

$$\hat{\tau}_i = \hat{M}_i \bar{\tau}_i \quad (12)$$

where sample mean $\bar{\tau}_i$ in cluster i is:

$$\bar{\tau}_i = \frac{1}{m_i} \sum_{j \in S_i} v_{ij} \quad (13)$$

where m_i is the number of sampled items in cluster i , M_i is the population total in cluster i and p_2 is the data item sampling rate.

Since $\hat{M}_i \sim \mathcal{NB}(m_i, p_2)$, estimated \hat{M}_i is:

$$\hat{M}_i = \frac{m_i}{p_2} \quad (14)$$

with variance:

$$\text{Var}(\hat{M}_i) = \frac{(m_i)(1-p_2)}{p_2^2} \quad (15)$$

The variance of sample mean in cluster i is:

$$\text{Var}(\bar{\tau}_i) = (1-p_2) \frac{s_i^2}{m_i} \quad (16)$$

The variance of estimated sum in cluster i is:

$$\begin{aligned} \text{Var}(\hat{\tau}_i) &= \hat{M}_i^2 \text{Var}(\bar{\tau}_i) + \bar{\tau}_i^2 \text{Var}(M_i) + \text{Var}(\hat{M}_i)\text{Var}(\bar{\tau}_i) \\ &= \left(\frac{m_i}{p_2}\right)^2 (1-p_2) \frac{s_i^2}{m_i} \\ &\quad + \frac{(m_i)(1-p_1)}{p_1^2} \left(\bar{\tau}_i + \frac{(m_i)(1-p_1)}{p_1^2}\right) \end{aligned} \quad (17)$$

Intra-cluster variance is:

$$\text{Var}_{intra} = \frac{1}{p_1} \sum_{i \in S} \text{Var}(\hat{\tau}_i) \quad (18)$$

The total variance is:

$$\begin{aligned} \text{Var}(\hat{\tau}) &= \text{Var}_{inter} + \text{Var}_{intra} \\ &= \text{Var}(\hat{\tau})_{srs} + \frac{1}{p_1} \sum_{i \in S} \text{Var}(\hat{\tau}_i) \end{aligned} \quad (19)$$

REFERENCES

- [1] F. T. Chong, M. J. R. Heck, P. Ranganathan, A. A. M. Saleh, and H. M. G. Wassel, "Data Center Energy Efficiency: Improving Energy Efficiency in Data Centers Beyond Technology Scaling," *IEEE Design & Test*, vol. 31, no. 1, 2014.
- [2] S. Agarwal, B. Mozafari, A. Panda, H. Milner, S. Madden, and I. Stoica, "BlinkDB: Queries with Bounded Errors and Bounded Response Times on Very Large Data," in *Proceedings of the EuroSys Conference*, 2013.
- [3] J. W. Liu, W.-K. Shih, K.-J. Lin, R. Bettati, and J.-Y. Chung, "Imprecise Computations," *Proceedings of the IEEE*, vol. 82, no. 1, 1994.
- [4] S. Misailovic, D. M. Roy, and M. C. Rinard, "Probabilistically Accurate Program Transformations," in *Proceedings of the International Static Analysis Symposium (SAS)*, 2011.
- [5] M. Zaharia, M. Chowdhury, T. Das, A. Dave, J. Ma, M. McCauly, M. J. Franklin, S. Shenker, and I. Stoica, "Resilient distributed datasets: A fault-tolerant abstraction for in-memory cluster computing," in *Presented as part of the 9th USENIX Symposium on Networked Systems Design and Implementation (NSDI 12)*. San Jose, CA: USENIX, 2012, pp. 15–28. [Online]. Available: <https://www.usenix.org/conference/nsdi12/technical-sessions/presentation/zaharia>
- [6] I. A. T. Hashem, I. Yaqoob, N. B. Anuar, S. Mokhtar, A. Gani, and S. U. Khan, "The rise of big data on cloud computing: Review and open research issues," *Information Systems*, vol. 47, pp. 98–115, 2015.
- [7] T. Akidau, R. Bradshaw, C. Chambers, S. Chernyak, R. J. Fernández-Moctezuma, R. Lax, S. McVeety, D. Mills, F. Perry, E. Schmidt, and S. Whittle, "The dataflow model: A practical approach to balancing correctness, latency, and cost in massive-scale, unbounded, out-of-order data processing," *Proc. VLDB Endow.*, vol. 8, no. 12, pp. 1792–1803, Aug. 2015. [Online]. Available: <http://dx.doi.org/10.14778/2824032.2824076>
- [8] J. G. Shanahan and L. Dai, "Large scale distributed data science using apache spark," in *Proceedings of the 21th ACM SIGKDD international conference on knowledge discovery and data mining*. ACM, 2015, pp. 2323–2324.
- [9] M. Armbrust, R. S. Xin, C. Lian, Y. Huai, D. Liu, J. K. Bradley, X. Meng, T. Kaftan, M. J. Franklin, A. Ghodsi *et al.*, "Spark sql: Relational data processing in spark," in *Proceedings of the 2015 ACM SIGMOD International Conference on Management of Data*. ACM, 2015, pp. 1383–1394.
- [10] J. Yu, J. Wu, and M. Sarwat, "Geospark: A cluster computing framework for processing large-scale spatial data," in *Proceedings of the 23rd SIGSPATIAL International Conference on Advances in Geographic Information Systems*. ACM, 2015, p. 70.
- [11] M. S. Wiewiórka, A. Messina, A. Pacholewska, S. Maffioletti, P. Gawrysiak, and M. J. Okoniewski, "Sparkseq: fast, scalable and cloud-ready tool for the interactive genomic data analysis with nucleotide precision," *Bioinformatics*, vol. 30, no. 18, pp. 2652–2653, 2014.
- [12] S. Lohr, *Sampling: Design and Analysis*. Cengage Learning, 2009.
- [13] M. Al-Kateb and B. S. Lee, "Adaptive stratified reservoir sampling over heterogeneous data streams," *Information Systems*, vol. 39, pp. 199–216, 2014.
- [14] S. Chaudhuri, G. Das, and V. Narasayya, "Optimized Stratified Sampling for Approximate Query Processing," *ACM Transactions on Database Systems (TODS)*, vol. 32, no. 2, 2007.
- [15] M. Al-Kateb and B. S. Lee, "Stratified reservoir sampling over heterogeneous data streams," in *Proceedings of the 22nd International Conference on Scientific and Statistical Database Management (SSDBM)*. Springer Berlin Heidelberg, 2010, pp. 621–639.
- [16] M. Thottethodi, T. Vijaykumar, M. Kulkarni *et al.*, "Stratified online sampling for sound approximation in mapreduce," 2015.
- [17] J. M. Hellerstein, P. J. Haas, and H. J. Wang, "Online Aggregation," in *Proceedings of the ACM SIGMOD International Conference on Management of Data (SIGMOD)*, 1997.
- [18] G. Kumar, G. Ananthanarayanan, S. Ratnasamy, and I. Stoica, "Hold 'em or fold 'em?: Aggregation queries under performance variations," in *Proceedings of the Eleventh European Conference on Computer Systems*, ser. EuroSys '16. New York, NY, USA: ACM, 2016, pp. 7:1–7:14. [Online]. Available: <http://doi.acm.org/10.1145/2901318.2901351>
- [19] X. Zhang, J. Wang, and J. Yin, "Sapprox: Enabling efficient and accurate approximations on sub-datasets with distribution-aware online sampling," *Proc. VLDB Endow.*, vol. 10, no. 3, pp. 109–120, Nov. 2016. [Online]. Available: <https://doi.org/10.14778/3021924.3021928>
- [20] I. Goiri, R. Bianchini, S. Nagarakatte, and T. D. Nguyen, "Approxhadoop: Bringing approximations to mapreduce frameworks," in *Proceedings of the Twentieth International Conference on Architectural Support for Programming Languages and Operating Systems*, ser. ASPLOS '15. New York, NY, USA: ACM, 2015, pp. 383–397. [Online]. Available: <http://doi.acm.org/10.1145/2694344.2694351>
- [21] J. Dean and S. Ghemawat, "Mapreduce: Simplified data processing on large clusters," in *Proceedings of the 6th Conference on Symposium on Operating Systems Design & Implementation - Volume 6*, ser. OSDI '04. Berkeley, CA, USA: USENIX Association, 2004, pp. 10–10. [Online]. Available: <http://dl.acm.org/citation.cfm?id=1251254.1251264>
- [22] D. L. Quoc, R. Chen, P. Bhatotia, C. Fetzter, V. Hilt, and T. Strufe, "Streamapprox: Approximate computing for stream analytics," in *Proceedings of the 18th ACM/IFIP/USENIX Middleware Conference*, ser. Middleware '17. New York, NY, USA: ACM, 2017, pp. 185–197. [Online]. Available: <http://doi.acm.org/10.1145/3135974.3135989>
- [23] M. Zaharia, T. Das, H. Li, S. Shenker, and I. Stoica, "Discretized streams: An efficient and fault-tolerant model for stream processing on large clusters," *HotCloud*, vol. 12, pp. 10–10, 2012.
- [24] A. I. McLeod and D. R. Bellhouse, "A convenient algorithm for drawing a simple random sample," *Journal of the Royal Statistical Society. Series C (Applied Statistics)*, vol. 32, no. 2, pp. 182–184, 1983.
- [25] J. S. Vitter, "Random sampling with a reservoir," *ACM Transactions on Mathematical Software (TOMS)*, vol. 11, no. 1, pp. 37–57, 1985.
- [26] M. D. Bankier, "Power allocations: determining sample sizes for sub-national areas," *The American Statistician*, vol. 42, no. 3, pp. 174–177, 1988.
- [27] B. P. Welford, "Note on a method for calculating corrected sums of squares and products," *Technometrics*, vol. 4, no. 3, pp. 419–420, 1962. [Online]. Available: <http://www.jstor.org/stable/1266577>
- [28] P. Berkhin, "A survey of clustering data mining techniques," in *Grouping multidimensional data*. Springer, 2006, pp. 25–71.
- [29] "MEDLINE Data," 2017, https://www.nlm.nih.gov/databases/download/pubmed_medline.html/.
- [30] D. Zhang, T. He, F. Zhang, M. Lu, Y. Liu, H. Lee, and S. H. Son, "Carpooling service for large-scale taxicab networks," *ACM Trans. Sen. Netw.*, vol. 12, no. 3, pp. 18:1–18:35, Aug. 2016. [Online]. Available: <http://doi.acm.org/10.1145/2897517>
- [31] D. Zhang, J. Huang, Y. Li, F. Zhang, C. Xu, and T. He, "Exploring human mobility with multi-source data at extremely large metropolitan scales," in *Proceedings of the 20th Annual International Conference on Mobile Computing and Networking*, ser. MobiCom '14. New York, NY, USA: ACM, 2014, pp. 201–212. [Online]. Available: <http://doi.acm.org/10.1145/2639108.2639116>
- [32] B. Liu, "Sentiment analysis and opinion mining," *Synthesis lectures on human language technologies*, vol. 5, no. 1, pp. 1–167, 2012.
- [33] (2011) Tweets 2011. <http://trec.nist.gov/data/tweets/>.
- [34] C. D. Manning, M. Surdeanu, J. Bauer, J. Finkel, S. J. Bethard, and D. McClosky, "The Stanford CoreNLP natural language processing toolkit," in *Association for Computational Linguistics (ACL) System Demonstrations*, 2014, pp. 55–60. [Online]. Available: <http://www.aclweb.org/anthology/P/P14/P14-5010>
- [35] J. Lin, "Cloud9: A Hadoop Toolkit for Working with Big Data," 2014, <http://lintoool.github.io/Cloud9>.
- [36] L. Page, S. Brin, R. Motwani, and T. Winograd, "The PageRank Citation Ranking: Bringing Order to the Web," Stanford InfoLab, Tech. Rep., 1999.
- [37] "Wikipedia database," http://en.wikipedia.org/wiki/Wikipedia_database_, 2016.
- [38] (2016) Wikipedia clickstream. https://meta.wikimedia.org/wiki/Research:Wikipedia_clickstream/.